AgustaWestland's Application of HMB to Simulate the Active Gurney Flap

Karl Baverstock
Principal Engineer
AgustaWestland, Aerodynamics Dept.
karl.baverstock@agustawestland.com

ABSTRACT

This paper describes the way in which the CFD solver HMB 2.0 has been used by AgustaWestland to calculate unsteady aerofoil characteristics in support of rotor performance calculations using blade element methods, and to provide local loads in support of structural design. Initial steady simulations and comparison between the predicted effects of Gurney flaps and those from wind tunnel testing are shown. The limitations of steady analysis, some of the key observations regarding the performance of Gurney flaps, and the effect of unsteady vortex shedding from them are noted. The method by which aerofoil external profiles have been modified to accommodate an active Gurney flap while maintaining the characteristics of the original section is described and the results presented. The significant computational effort required simulating each point as a time accurate simulation at fixed incidence over the range of incidence and Mach number possible in flight is noted and a novel method of look-up table generation via low ramp-rate CFD simulations is described. Beyond simple pseudo steady data table generation, comparisons are made between dynamic stall predictions for the original clean aerofoil and the modified aerofoil with Gurney flap. These justify the use of simple first generation dynamic stall prediction tools for Gurney flap configurations. Finally, simulations of the dynamic deployment of a Gurney flap on an aerofoil with varying incidence and Mach number, representative of operating conditions on a main rotor and the provision of local aerodynamic loads in support of detailed design are presented.

NOTATION

C	Aerofoil chord.
C_D	Aerofoil drag coefficient.
C_L	Aerofoil lift coefficient.
C_m	Aerofoil pitching moment coefficient.
C_{m0}	Aerofoil pitching moment coefficient at zero lift.
M	Freesteam Mach number.
S	Class function transformation of aerofoil thickness.
St	Strouhal number.
t	Time.
t	Aerofoil thickness.
t_{te}	Aerofoil thickness at its trailing edge.
U	Freestream velocity.
x	Distance aft of leading edge.
α	Aerofoil incidence.
α_0	Aerofoil incidence at zero lift.
$\dot{\theta}$	Aerofoil pitch rate.
ψ	Rotor azimuth angle.

1. INTRODUCTION

The ultimate goal of the Clean Sky Joint Technology Initiative (JTI) is to reduce external noise, and provide cleaner, more efficient power use. This will contribute to the top-level Advisory Council for Aviation Research and Innovation in Europe (ACARE) 2020 goals to halve emitted carbon dioxide, cut specific emissions of nitrogen oxides by 80% and halve perceived noise produced by the European aviation sector. In the initial phase of the Clean Sky JTI Green Rotorcraft (GRC) programme of activities, AgustaWestland (AW) and several European research bodies reviewed the possible active rotor technologies that can delay retreating blade stall[1]. This review was assessed by AW from an industrial implementation perspective. This included consideration of the ease of integration and actuation of the active technologies and concluded in the selection of the Active Gurney Flap (AGF) for further consideration. The ultimate result of these efforts by AW and its partners will be the flight test demonstration of an AGF on a modified AW139,

which aims to demonstrate reduced main rotor power at high thrust coefficients. In future rotor designs, it is hoped to alleviate retreating blade stall through redistribution of lift, and hence allow smaller, more efficient rotors to be utilised.

By the time the AGF had been selected for the Clean Sky GRC programme of work, AW had entered into a collaborative agreement with the University of Liverpool, to establish a word class centre of expertise: the AW and University of Liverpool Applied Research Centre (AWL-ARC). Via the AWL-ARC, the University of Liverpool CFD Laboratory has been developing the Helicopter Multi-Block 2.0 (HMB 2.0) CFD tool for AW, specifically tailored to the needs of the AW Aerodynamics department. This CFD code solves the unsteady Reynolds-averaged Navier-Stokes equations on multi-block structured mesh topologies, using a cell-centred finite-volume method for spatial discretisation and an implicit dual-time stepping method, based on Jameson's pseudo-time integration approach for unsteady simulations. Development of HMB has been documented previously[2], including its application to Gurney flaps[3][4].

2. INITIAL COMPARISON WITH TEST DATA

In the early 1990's, Westland Helicopters Ltd. had investigated the possibility of using a fixed Gurney flap on a high performance helicopter rotor aerofoil. This resulted in wind tunnel tests in the ARA 18" x 8" Two-Dimensional wind tunnel to establish the aerodynamic characteristics of the RAE 9645 aerofoil with fixed Gurney flap at the trailing edge[5]. These data were used for initial predictions of the benefits of the AGF for helicopter main rotors.

Within AW there was already some experience of running HMB 1.4 and the Aerodynamics department was engaged in developing a method for the automated generation of aerofoil polars using Excel macros, ICEM replay files and shell scripts to run HMB and collect the data in a single text file. This was aimed at complementing the existing capability using the MSES commercial aerofoil analysis suite of codes. Although a small cluster was available, this had fewer cores than some of today's high-end work stations, limiting what could be achieved. The GRC programme of work provided the opportunity to use HMB in routine aerofoil studies and highlighted the requirement for an additional capability with respect to modelling the Gurney flap.

Initially, AW requested the addition of a new boundary condition in HMB, whereby both sides of a block boundary would be flagged as a wall, with halo cells on either side. By splitting a c-mesh around the aerofoil at the height of the Gurney flap and flagging the block boundary perpendicular to the chord at the Gurney flap location with this new 'fake' wall condition, a simple representation of a fixed Gurney flap could be achieved. These cases were difficult to converge using steady simulations, not only near maximum lift, but also at low incidence, due to the intrinsically unsteady nature of the flow. However, given the limited computational resources available the results were encouraging and judged to be the best practicable approach to providing engineering data in the short term. These results are plotted in comparison with wind tunnel test data in Figure 1. Recently, with significantly improved computational facilities at AW, these cases have been repeated using unsteady simulations. The unsteady simulations give similar results to the steady simulations, but with a significant improvement in the regularity of the trends shown in Figure 1. One exception is the drag increase due to Gurney flap deployment, which is slightly lower than that calculated from wake measurements in the wind tunnel test for the steady simulations, but up to 14 counts higher than measured for the unsteady simulations. Another interesting feature is that at Mach 0.3 and 0.7 the increase in maximum lift coefficient due to the Gurney flap is greater than at Mach 0.5. At Mach 0.3 the predicted stalling is progressive from the trailing edge, and at Mach 0.7 it originates from the foot of the shock at the end of the supercritical region on the upper surface, whereas at Mach 0.5 the predicted separation originates at the trailing edge, but a bubble at the foot of the shock is also present.

This technique was applied to several different helicopter main rotor aerofoils, and the fixed trailing edge Gurney flap was compared with the effect of a 15% chord plain flap on the same aerofoil at typical main rotor conditions. In these investigations it was concluded that the Gurney flap has a powerful effect on zero lift angle and pitching moment and was more powerful than the plain flap, although flap angles were limited to the range where separation does not occur. The Gurney flap also had greater potential for increasing the maximum lift coefficient of the aerofoil. On the other hand, the Gurney flap always produced a significant drag penalty, such that for a given lift coefficient, the drag of the aerofoil was always higher than that of the clean or flapped aerofoil, except close to or beyond the maximum lift coefficient of the clean or flapped aerofoil. This contrasts with the example shown by Liebeck[6], where the drag of an

unconventional aerofoil is reduced by the application of a Gurney flap.

3. AEROFOIL MODIFICATION

Following initial structural design studies, it was hoped that a conventional helicopter rotor blade aerofoil could be made to accommodate a retracted, linearly actuated, 2% chord Gurney flap by local thickening of the aerofoil to 3% chord at the 95% chord location, maintaining the tab feature used to bond the upper and lower skins. However, it became clear that the high curvature required to achieve this would cause a separation ahead of the trailing edge, significantly reducing the lift curve slope of the aerofoil, altering its pitching moment characteristics and increasing drag. The solution adopted was to thicken the trailing edge of the aerofoil, sacrificing drag to maintain the lift and pitching moment characteristics of the datum aerofoil. This requirement to maintain the datum aerofoil characteristics aimed to provide consistency with the aerodynamic performance of the unmodified blade and therefore simplify the process by which the modified blade could be accepted for flight test. The decision did however preclude the possibility of modifying the aerofoil to create a design which depended on the Gurney flap being deployed to achieve the maximum possible lift coefficient.

Partially following the Class function / Shape function Transformation (CST) technique presented by Kulfan[7], The half thickness of the aerofoil was transformed by the class function so that:

(1) $$S = \frac{\left(\frac{t}{2C}\right) - \left(\frac{t_{te}}{2C}\right)}{\sqrt{\frac{x}{C}\left(1-\frac{x}{C}\right)}}$$

An iterative process was followed whereby the trailing edge thickness was guessed, attempting to match the maximum lift coefficient of the original aerofoil, and hence the value of transformed geometry was fixed at 95% chord. Ahead of 55% chord the geometry was fixed so that the rear spar of the donor blade would not be altered. Fitting a third order curve that matched the slope of the transformed geometry at 55% chord and was constrained at 95% chord left one degree of freedom, which defined the value of the transformed geometry at the trailing edge, and hence the aerofoil closure, or boat-tail angle which directly controlled the lift curve slope.

This process was followed with a NACA0012 aerofoil in order to generate a generic AGF aerofoil section which could be used to provide validating wind tunnel test data. In this case a suitable geometry, shown in the upper part of Figure 2, was found after four attempts to match the datum aerofoil lift characteristics at Mach 0.1, Reynolds number 1.0×10^6, the assumed conditions for low speed wind tunnel testing. The resulting effects on the aerofoil performance predicted by MSES and by steady HMB simulations are shown in Figure 3. Note that the MSES simulations have been run with both transition free, assuming critical amplification factor of 9, and with transition fixed at 5% chord. By comparison the HMB simulations have used Menter's k−ω SST turbulence model with a fully turbulent boundary layer. These indicate an acceptably small drag penalty for the clean aerofoil and that the lift curve slope has been preserved. The maximum lift coefficient has been slightly increased according to these predictions, suggesting that the trailing edge thickness could be reduced slightly. Given the difficulty in reliably predicting maximum lift coefficient, a little conservatism seemed justified.

The process was repeated for the ARO212 main lifting aerofoil used on the AW139 helicopter. Initially a nominally 2% AGF was accommodated by thickening to 3% chord at 95% chord, blending with the original geometry at 55% chord to produce the AW120_001 aerofoil. Later, a more minor modification was made, thickening to 2% chord at 95% chord, the AW120_002. It was found that the smaller change to the aerofoil made it possible to move the point where the blend with the original aerofoil was made to 78% chord with only a small adverse effect on the curvature of the aerofoil surfaces. This kept the geometry the same as that of the original ARO212 until aft of a break in the structure of the donor blade to be used for flight testing. For both of these aerofoils a very minor modification to the camber line was necessary to maintain the zero lift pitching moment of the original aerofoil.

4. UNSTEADY SIMULATION

Liebeck[6] hypothesized a mechanism whereby three vortices exist adjacent to the Gurney flap, one upstream and two downstream. Subsequent researchers have measured the flow, and at the Reynolds numbers of interest for helicopter main rotor design, unsteady vortices are shed from the Gurney flap, for example in References 8, 9 and 10. It was recognised that despite the reasonable agreement between the wind tunnel test data available for the RAE9645 aerofoil and steady state HMB simulations, there could well be a discrepancy between the flow modelled in the simulation and the real flow behind the Gurney flap. It was also clear that AW lacked the capability to correctly simulate transient cases where the Gurney flap was being deployed and retracted. In

response to this, AWL-ARC was asked to investigate ways in which the unsteady AGF could be modelled. This resulted in the HMB developments described in Reference 3.

Initial unsteady work involved running fixed incidence cases with a fixed Gurney height. To do this the mesh needed to be fine enough and the time step needed to be small enough to resolve the unsteady flow. The highest frequencies and smallest features are found on the blunt trailing edge aerofoil with the Gurney flap retracted, and therefore time step sensitivity studies have been conducted for this configuration, as shown in Figure 4. This revealed that a time step, non-dimensionalised by chord and freestream velocity, $\frac{\Delta t\, U}{C} = 0.002$, was necessary to resolve the trailing edge vortex shedding. It also showed that the predicted drag rise due to thickening the aerofoil was about 50% greater than had been predicted by steady HMB and MSES simulations, although this was still considered acceptable.

Using the approach of modelling a Gurney flap using a time variable viscous wall boundary condition across a block face it was possible to model the extension and retraction of the device. Figure 5 shows predictions of the effect of a rapid deployment and retraction of the Gurney flap on the modified NACA0012 aerofoil at wind tunnel conditions. In this simulation the Gurney is extended or retracted in 5ms with the cycle repeated every 40ms. There is an initial rapid response to the Gurney flap deployment or retraction, followed by an asymptotic rise or fall to steady state values due to the vorticity shed in the wake. When the deployment of the Gurney flap becomes rapid, a short period transient undershoot and overshoot is seen in the lift and pitching moment characteristics, probably due the formation of a strong discrete vortex. Testing at the University of Twente has been conducted to validate these predictions. The data are not yet analysed and available for comparison, but initial observations noted whistles from the test rig. An investigation of the frequencies in the wake to be published by Van't Hoff[11] indicates that these frequencies are close to those predicted by HMB simulations of the aerofoil in free-air produced prior to the test. A comparison of the Strouhal number based on the sum of the trailing edge thickness and the Gurney deployment height is given in Figure 5. The value is slightly less than the value of 0.15 reported for a simple trailing edge Gurney flap on the NACA0015 aerofoil[10]. The match to test data is good with the AGF retracted, but poorer when extended. This may be improved by including the tunnel boundaries and real details of the experimental set-up in the simulation. From these studies it was deduced that a blade element model which included a method to capture the lag due to vorticity shed in the near wake from a pitching aerofoil would be capable of predicting the effects of Gurney flap deployment, providing there was no requirement to capture the vortex shedding frequencies and higher.

A significant part of the work of the AW Aerodynamics department is in providing aerofoil characteristics to the Rotor Dynamics and Flight Mechanics departments for use in their blade element models. In the past this has been done by wind tunnel testing, or sometimes in situations where a new aerofoil differs only slightly from an older one, by making small adjustments to data for previous aerofoil designs on the basis of MSES simulations. With the introduction of HMB 2.0 it was possible to provide the required data for the modified design ahead of testing. Unsteady simulations with a fixed Gurney flap at fixed incidence showed that, in contrast with the fixed Gurney flap at the thin trailing edge, it was necessary to perform unsteady simulations to correctly predict the drag, and to a lesser extent lift and pitching moment, of the aerofoil. This is due to the lower time averaged pressure calculated behind the AGF in unsteady simulations compared with steady simulations. This acts like a base pressure across the thickened aerofoil section. In some conditions it was also found that a considerable time was necessary to allow the forces and moments to settle to a periodically repeating pattern.

It was clear that to perform sufficient simulations to capture the lift, pitching moment and drag characteristics of the aerofoil would require a very significant computational effort. To reduce this, a novel approach was taken to calculating these polars. The aerofoil was simulated as a continuous ramp about the quarter chord, starting well below zero lift and ending above the stall. The ramp rate was increased from zero at the start of the simulation, to avoid an impulse being introduced, and then increased to a non-dimensional rate of $\frac{tU}{C} = 0.002 rad$. The results of the simulation were then approximately corrected back to steady state conditions for the non-circulatory effects induced by the pitching motion[12] and assuming only a steady rotation of the flow at the aerofoil due to the vorticity shed in the wake[13].

(2) $$\propto_{corr} = \propto + \frac{\dot{\theta} C}{U} \frac{2.3715}{(1-M^2)}$$

(3) $$C_{Lcorr} = C_L + \frac{\dot{\theta} C}{U} \frac{\pi}{\sqrt{1-M^2}}$$

(4) $$C_{mcorr} = C_m + \frac{\dot{\theta}C}{U}\frac{\pi}{8\sqrt{1-M^2}}$$

(5) $$C_{Dcorr} = C_D - \frac{\dot{\theta}C}{U}\frac{2.3715}{(1-M^2)}C_L$$

As an example, HMB simulations of the NACA0012 aerofoil are compared with experimental data[14] in Figure 6. For this aerofoil the steady and unsteady simulations give the same results where the flow is fully attached. Near maximum lift the unsteady results are much closer to the experimental data than the steady results; however, the movement of the separation point from near the trailing edge to the leading edge is not captured. This is possibly due to differences in the boundary layer state close to the leading edge between the simulation and the test. The ramping simulation should give the same results as the unsteady fixed angle simulations if the corrections were exact. Figure 6 shows that following correction the ramping simulation gives a slightly optimistic prediction of the maximum lift coefficient. The rotation applied to account for the shed vorticity in the wake is slightly too large and over corrects the drag. These differences are small compared with the effects of the Gurney flap. On this basis it was judged an acceptable method for calculating incremental changes to aerofoil polars. This was done for several different Gurney extensions over the full range of Mach numbers on the rotor, and more rapidly than could otherwise be done with a limited number of cores available.

Once data had been generated for low ramp rates to populate tables of steady state aerofoil characteristics, it was a small step to increase the ramp rate and investigate the effect of the deployed AGF on dynamic stall characteristics. An example is shown in Figure 7, which indicates that the 1.9 chord length delay for pitching moment delay and 3 chord length normal force delay assumed in the original Beddoes' dynamic stall delay model[13] are equally applicable for an aerofoil with an AGF flap as for an aerofoil with a conventional tailing edge.

The final aerofoil performance aspect investigated using HMB was to simulate the modified aerofoil with an AGF as it pitches and accelerates around the azimuth, the so called dM/dt approach. Figure 8 shows a simulation of an aerofoil as its Mach number and incidence vary around the azimuth while a 1% chord active Gurney flap deploys and retracts, and compares the lift with that predicted by CAMRAD[15] using aerofoil characteristics from pseudo steady look-up tables in C81 format. The CAMRAD simulation was used to obtain the aerofoil incidence for the HMB simulation. High frequency unsteady forces and moments are predicted at the front and rear of the disc where there are moderate incidence and Mach number, and a strong nose down pitching moment is also noted at the same locations. The lift coefficient results are non-dimensionalised by the maximum lift coefficient of the unmodified aerofoil low-Mach number and the increase in maximum available lift which is now used on the rotor is clearly shown. The same simulation was later repeated using the Chimera, or overset mesh technique. This was initially developed in the UK Technology Strategy Board (TSB) funded Rotorcraft Technology Validation Programme (RTVP) programme, and modified under AWL-ARC to specifically enable the localisation of Gurney flaps. This later Chimera simulation was primarily used to obtain loads on the AGF in typical flight conditions, but was also useful to ensure that there were no significant performance penalties due to air flowing in the clearance gaps between the AGF and rotor structure. Mach number contours around the aerofoil with the Chimera representation of the AGF and simplified cavity are also shown in Figure 8.

5. LOADS PREDICTION

In the detailed design phase of the flight test rotor blade, the HMB CFD capability was used to provide unsteady pressure distributions on the blade surface and within the cavity containing the AGF. These were necessary for the structural design of the rear portion of the blade, and of the Gurney flap and its actuation mechanism. Initially, the work was done using multi-block structured meshes to represent section through the rotor and AGF in a fixed position. Later, as mentioned previously, the pressure distributions in typical flight conditions were calculated using Chimera simulations. Figure 9 presents results for the normal and axial forces on the fixed AGF during a ramp with 1% extension. Note that the axial force is non-dimensionalised by the freestream dynamic pressure and the exposed AGF height, whereas the normal force is non-dimensionalised by the AGF thickness. The axial loads are largely independent of the shape of the portion of the Gurney flap inside the blade cavity. On the other hand, the normal or vertical loads are strongly dependent on the size of the gaps between the lower surface skins and the AGF as these act as throats controlling the flow-rate into and out of the cavity, altering the static pressure within the structure. The detail of the design of the portion of the AGF inside the cavity also affects the normal forces. The unsteady vortex shedding from the aerofoil forms a significant part of the load. However, at the highest loadings, i.e. where the aerofoil is stalled or

approaching the stall, this unsteady loading does not exist.

6. CONCLUSIONS AND FUTURE WORK

The work presented in this document shows how a concerted effort over several years, co-ordinating different streams of research funding, has provided new capabilities in HMB. It also shows how the Clean Sky GRC programme of work has provided the opportunity to exploit these capabilities in-house, in support of a real flight test programme.

From unsteady two-dimensional aerofoil results it is deduced that a blade element method which includes a near wake model and conventional dynamic stall model will also be equally able to model the performance of a rotor with an AGF as it is a conventional rotor, providing the steady characteristics of the AGF aerofoil in the conditions present on the rotor are available.

The effect of unsteady vortex shedding on aerofoil characteristics has been shown, and the computational effort required to capture these effects noted. While the presence of the predicted unsteady vortex shedding has been validated in low-speed wind tunnel tests of the modified NACA0012 aerofoil, a full comparison between the test data and predictions is yet to be done. More complex simulations including representations of the wind tunnel boundaries may well be necessary to obtain a good match. It is worth noting that the trailing edge thickness to chord ratio of the modified NACA0012 aerofoil, 1.35%, is thinner than that of many root aerofoils used on helicopters and propellers without problems.

The same aerofoil will be used for model rotor tests in the Politecnico di Milano wind tunnel next year. In this case the Reynolds Number is lower and HMB does not predict unsteady vortex shedding from the clean aerofoil. With the Gurney flap fully deployed, however, vortex shedding is predicted for the two-dimensional aerofoil. It is not certain that the same coherent vortex structure will exist in a rotating frame of reference, and it may be that the separated flow regions are modified, similar to the way in which trailing edge stall is delayed on the thick root sections of propellers. These wind tunnel tests will provide useful information regarding performance of the Gurney flap with three dimensional effects in the rotating environment. Although forward flight simulations with an active Gurney flap have been performed by the University of Liverpool[4], AW has not attempted this yet. In the future it would be useful to perform three dimensional rotating simulations in HMB with fine enough meshes and small enough time steps to accurately simulate the vortex structure from a thick trailing edge or Gurney flap.

There is still some uncertainty regarding drag prediction with an AGF. Testing at near full-scale in the CIRA icing wind tunnel, to be completed in early 2015, will provide data with which to validate the drag predictions from HMB.

ACKNOWLEDGEMENTS

The reported activities have been funded by the Clean Sky Joint Undertaking, and also supported by the AWL-ARC. The author would particularly like to thank Professor George Barakos and Dr. Mark Woodgate for their help and training in the use of HMB.

COPYRIGHT STATEMENT

REFERENCES

[1] Maybury, W.J., Carrus, M., Visingardi, A., Donelli, R., van't Hoff, S.C., Bakker, R.J.J., Hakkaart, J.F., Betran, J., Pavel, M., de Boer, A., Paternoster, A.R.A., de Jong, P., "GRC1.1 Technology Review Document", GRC/RP/1.1/31005, 2010.

[2] Barakos, G., Steijl,R., Badcock, K., and Brocklehurst, A., "Development of CFD Capability for Full Helicopter Engineering Analysis.", 31st European Rotorcraft Forum, 13-15 September 2005, Florence, Italy.

[3] Woodgate, M., and Barakos, G., "Rotor Computations with Active Gurney Flaps.", 38th European Rotorcraft Forum, 4-6 September 2012, Amsterdam, Netherlands.

[4] Pastrikakis, V., Steijl R. and Barakos, G., Computational Analysis of the W3 Sokol Rotor with Gurney Flaps, 39th European Rotorcraft Forum 3-6 September 2013, Moscow, Russian Federation.

[5] Humphreys, C. and Smith, L., "Steady State Results from Tests in the ARA Two-Dimensional Wind Tunnel on the RAE 9645

Aerofoil Section with a Trailing Edge Device.", ARA Model Test Note G71/2, September 1993.
[6] Liebeck, R.H., “Design of Subsonic Airfoils for High Lift,” Journal of Aircraft, Vol. 15, No. 9, 1978, pp. 547–561.
[7] Kulfan, B.M, "A Universal Parametric Geometry Representation Method." AIAA Paper 2007-62, January 2007.
[8] Zerihan, J. and Zhang, X., “Aerodynamics of Gurney Flaps on a Wing in Ground Effect,” Journal of Aircraft, Vol. 39, No. 5, 2001, pp. 772–780.
[9] Hage, W., Meyer, R. and Schatz, M., "Comparison of experimental and numerical work on three dimensional trailing edge modifications on airfoils.", Integrating CFD and Experiments in Aerodynamics, September 2005, RCMS Shrivenham.
[10] Troolin, D.R., Longmire, E.K. and Wing T. Lai, W.T.,” The Effect of Gurney Flap Height on Vortex Shedding Modes Behind Symmetric Airfoils,” 13th International Symposium on Applications of Laser Techniques to Fluid Mechanics, Lisbon, Portugal, 26-29 June, 2006.
[11] van ‘t Hoff S., Tuinstra, M. and van Rooij, M., “Time-Resolved Stereo PIV Measurements of an Active Gurney Flap System”, 40th Eurpoean Rotorcraft Forum, September 2014, Southampton, UK.
[12] Theodorsen, T. "General Theory of Aerodynamic Instability and the Mechanism of Flutter." NACA TR 496, 1935.
[13] Chan, W., and Perry, J., "Use of aerofoil section dynamic stall synthesis methods in rotor design." The Aeronautical Journal, Vol. 116 No. 1179, May 2012.
[14] Ladson, C.M., "Effects of Independent Variation of Mach and Reynolds Numbers on the Low-Speed Aerodynamic Characteristics of the NACA0012 Airfoil Section." NASA TM4074, October 1988.
[15] Johnson, W.,"CAMRAD/JA A Comprehensive Analytical Model of Rotorcraft Aerodynamics and Dynamics." Vol. II: User's Manual, 1988.

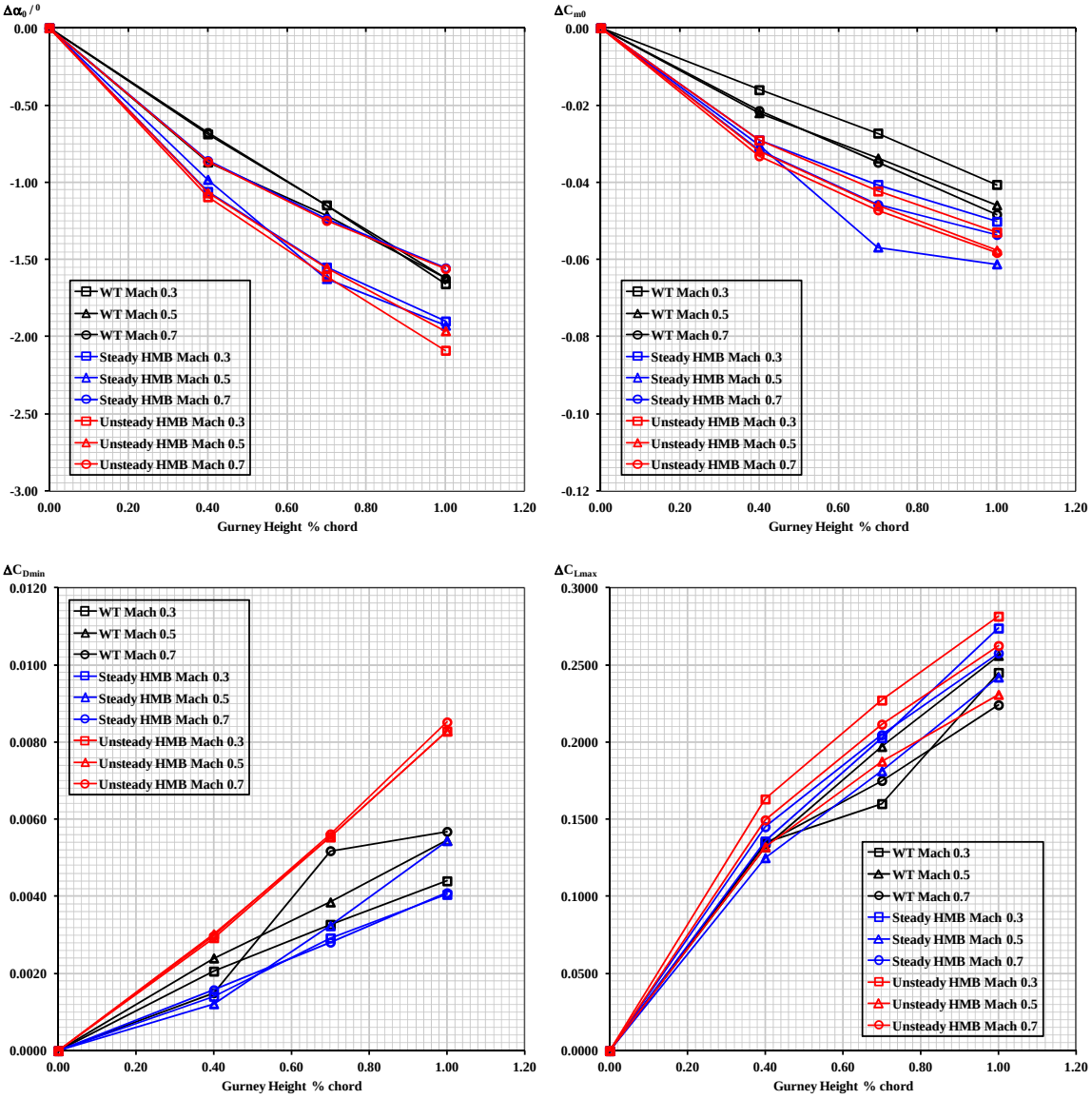

Figure 1: Effect of a Fixed Trailing Edge Gurney Flap on the RAE9645 Aerofoil Compared with Steady and Unsteady HMB Simulations.

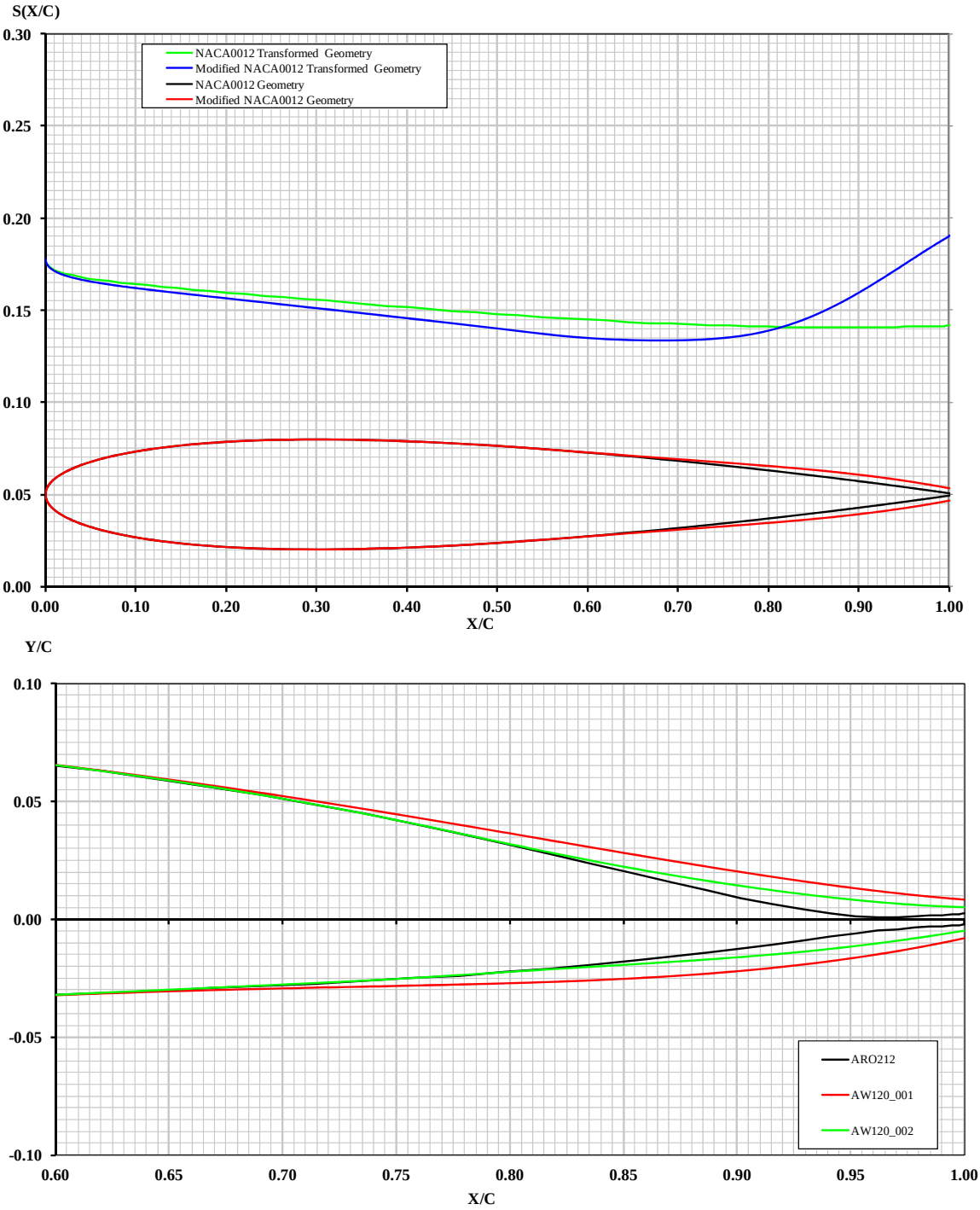

Figure 2: Geometry Modification of NACA0012 Aerofoil to Accommodate Active Gurney Flap (Top) and to the ARO212 Aerofoil to Accommodate a 2% and 1% Chord AGF at 95% Chord (Bottom).

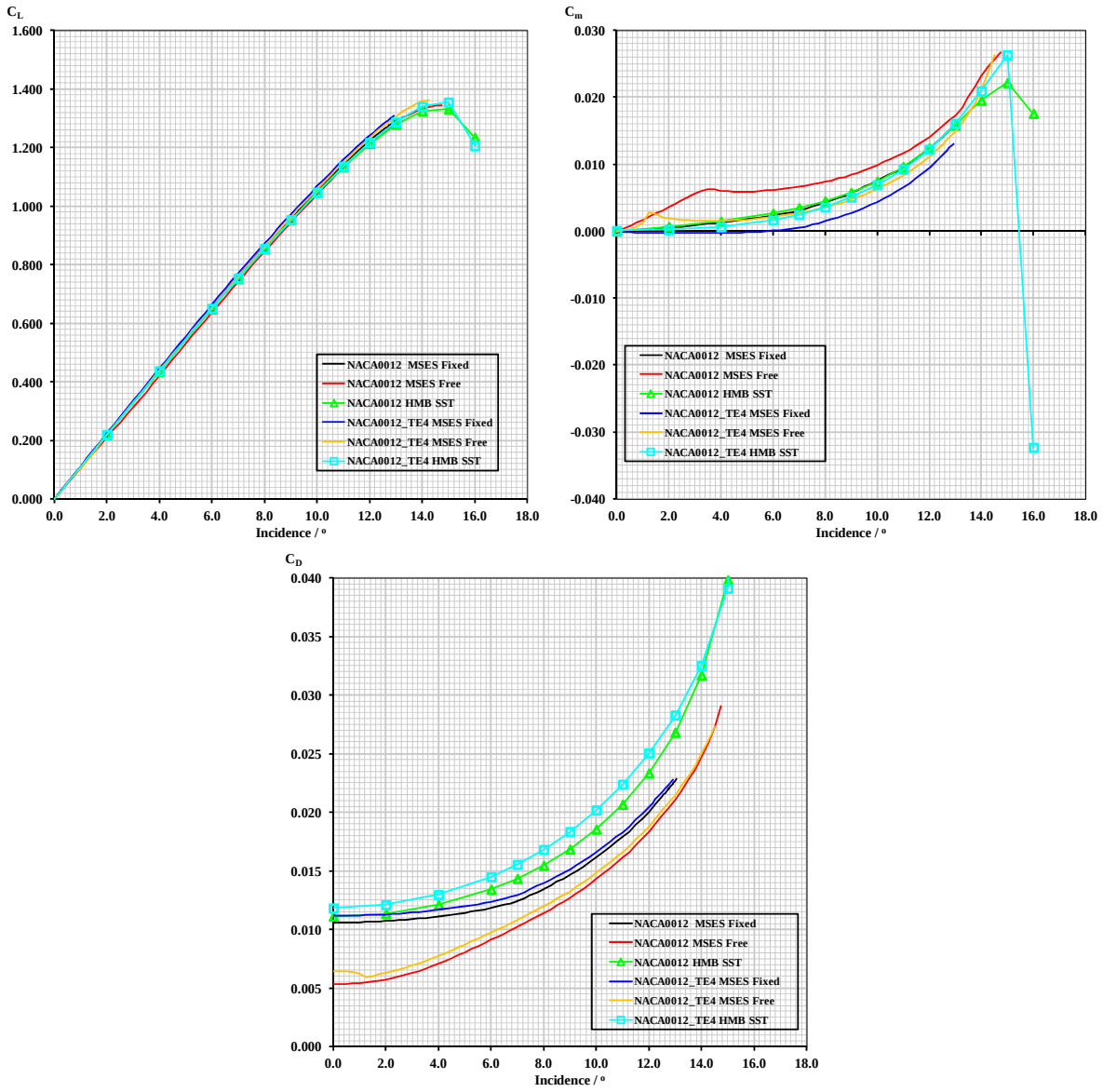

Figure 3: Comparison of MSES simulations with Transition Fixed and Free and HMB Predictions of the Effect of Trailing Edge Thickening to Accommodate an Active Gurney Flap.

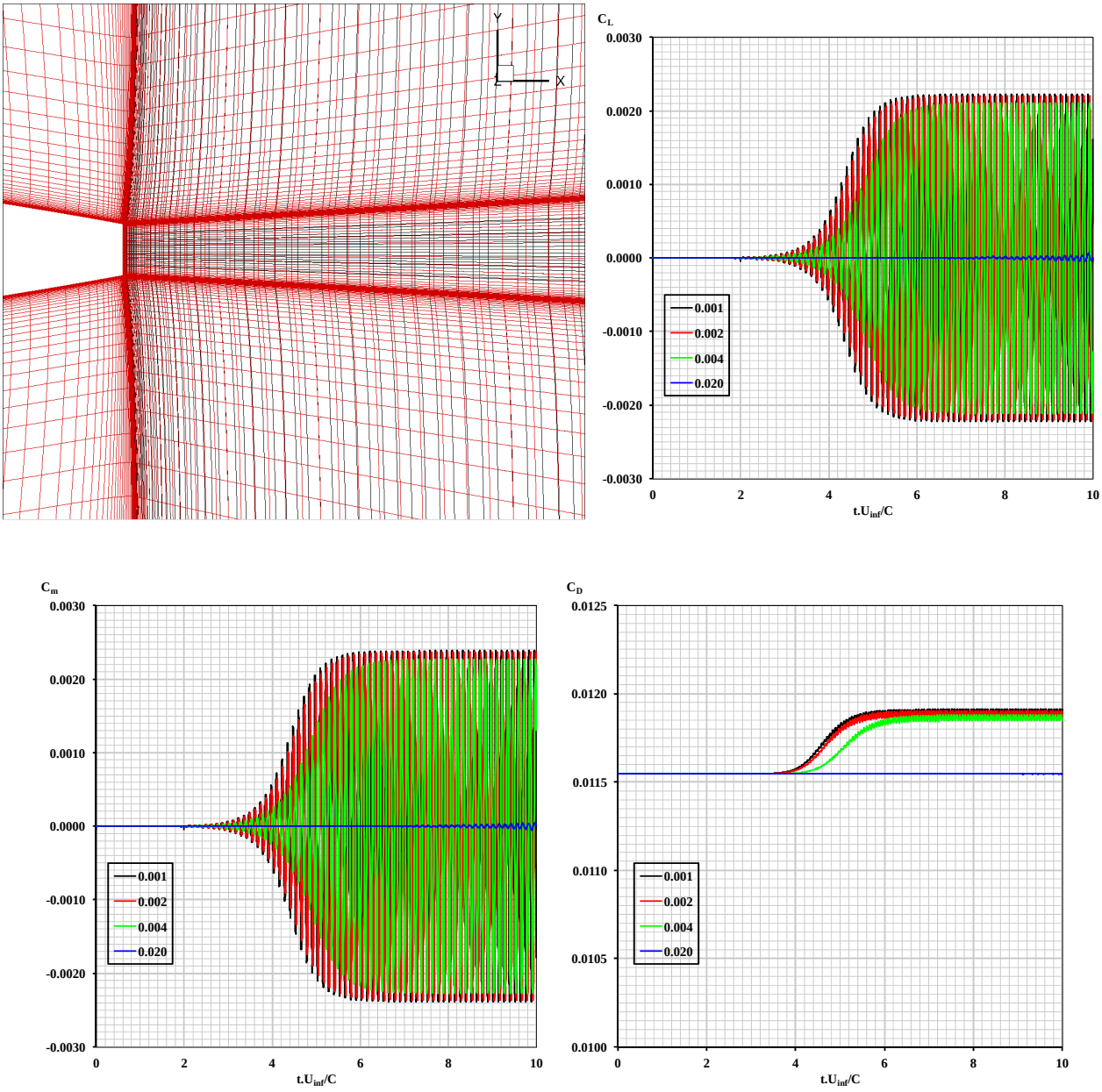

Figure 4: Comparison between Mesh too Coarse in the Wake Region to Capture Unsteady Vortex Shedding (Red) and Mesh Sufficiently Fine to Resolve Unsteady Features (Black), and the effect of Time Step (Δt.U/C) on Force and Moment Resolution for the Modified NACA0012 Aerofoil.

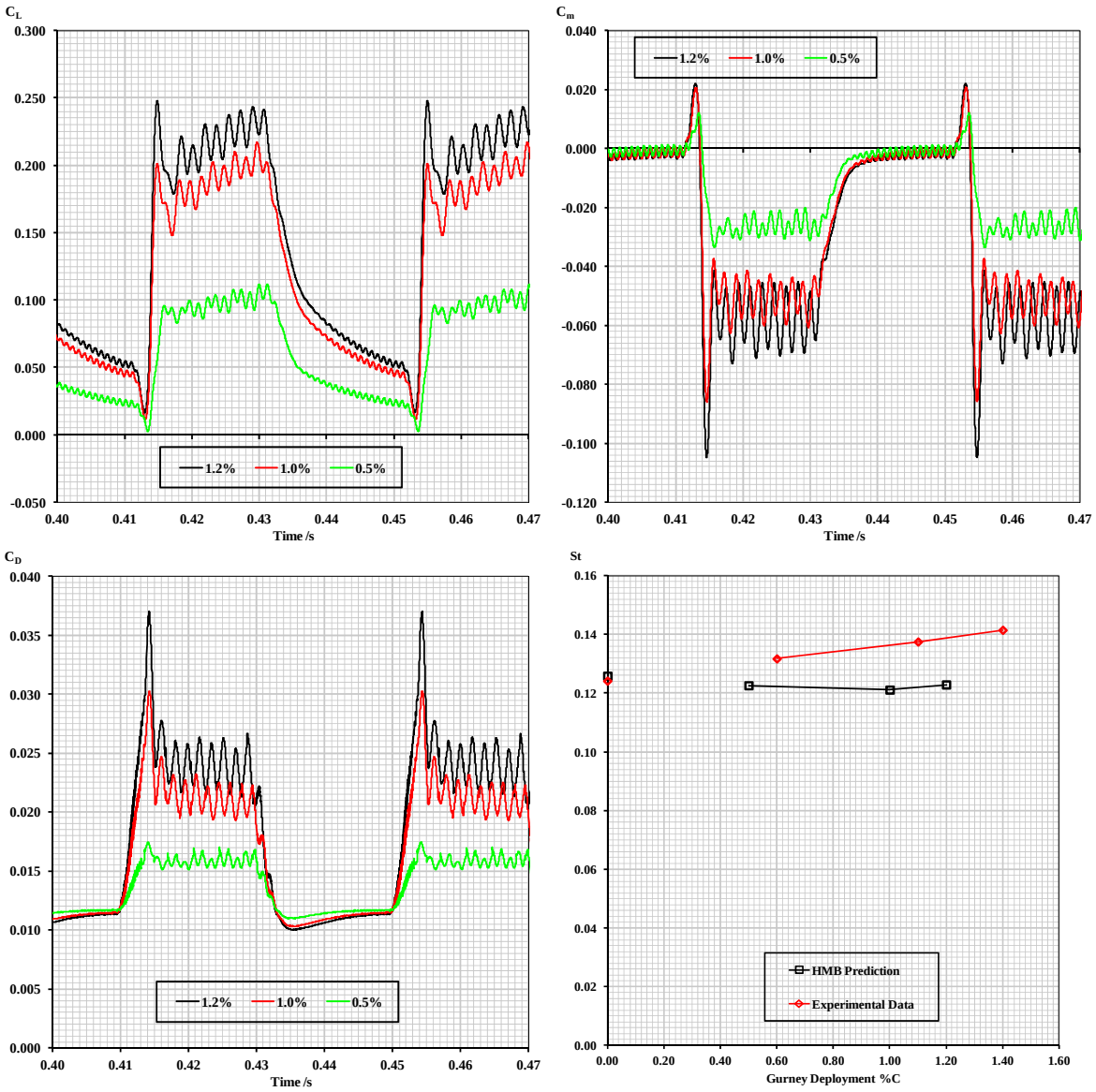

Figure 5: Predicted Forces and Moments due to Rapid Deployment of the Gurney Flap to Three Different Extents on the Modified NACA0012 Aerofoil and First Estimates of Predicted Vortex Shedding Strouhal Number Based on Trailing Edge Thickness Plus Gurney Deployment Height Compared with Wind Tunnel Test Results.

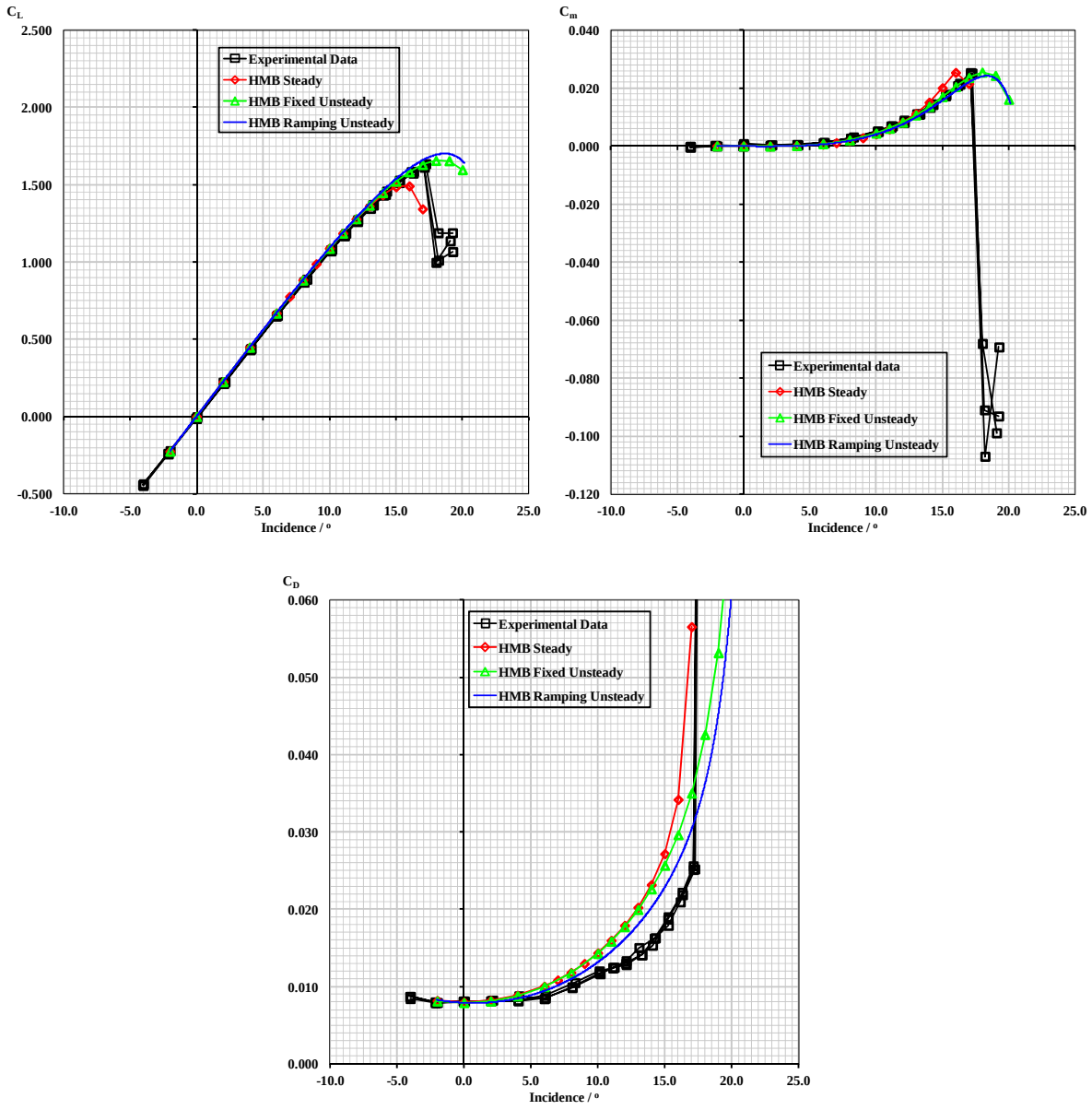

Figure 6: Comparisons between Wind Tunnel Test Data, Steady HMB Simulations, Unsteady Fixed Incidence HMB Simulations, and a Low Ramp Rate Simulation, Corrected to Steady Conditions, for the NACA0012 Aerofoil at Mach 0.15 and Reynolds Number 6×10^6.

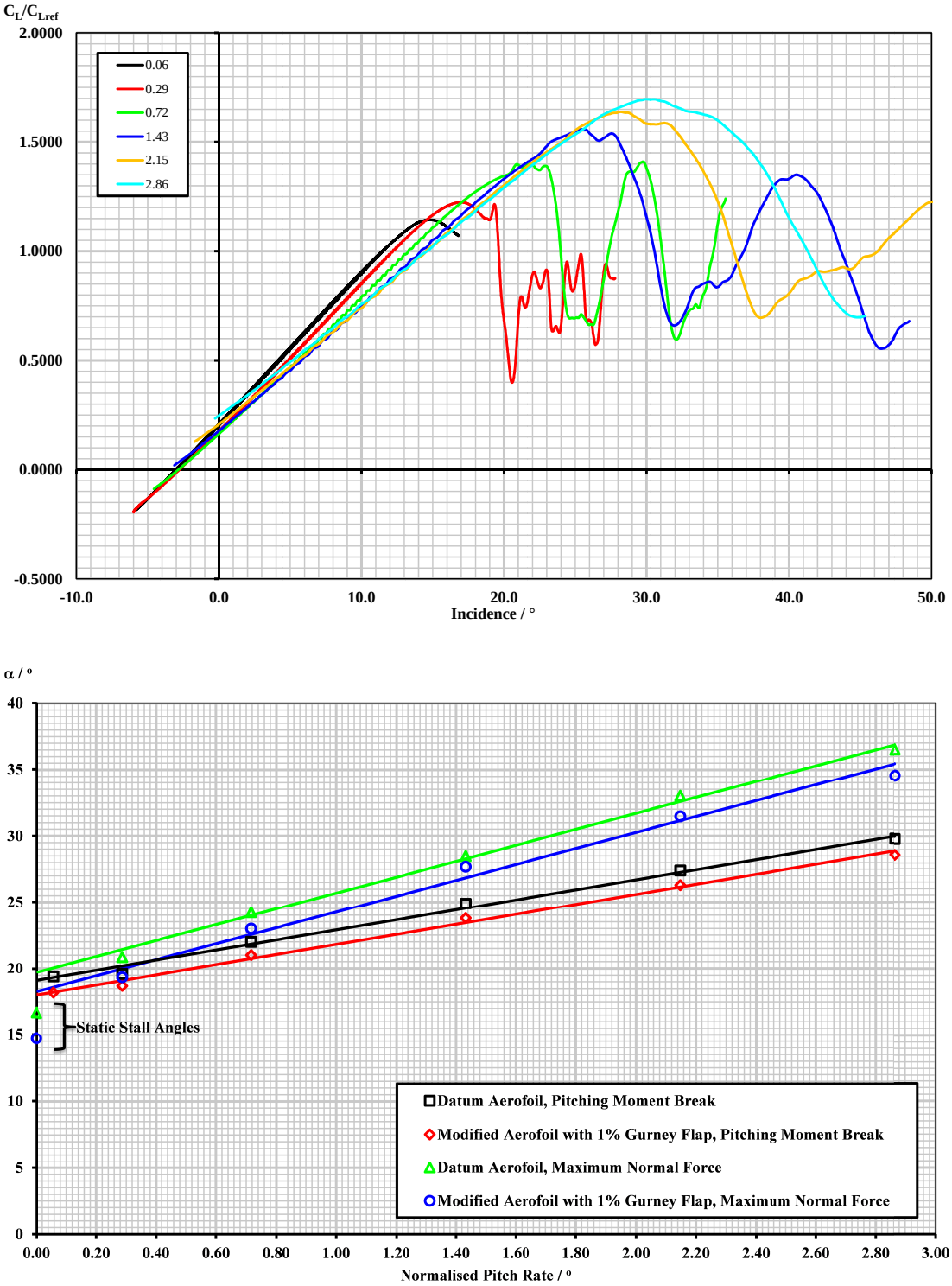

Figure 7: Comparison of Dynamic Stall Characteristics of Datum Aerofoil and Modified Aerofoil with 1% Gurney Flap at 95% Chord for Various Normalised Pitch Rates $\left(\frac{\dot{\theta}C}{2U}\right)$.

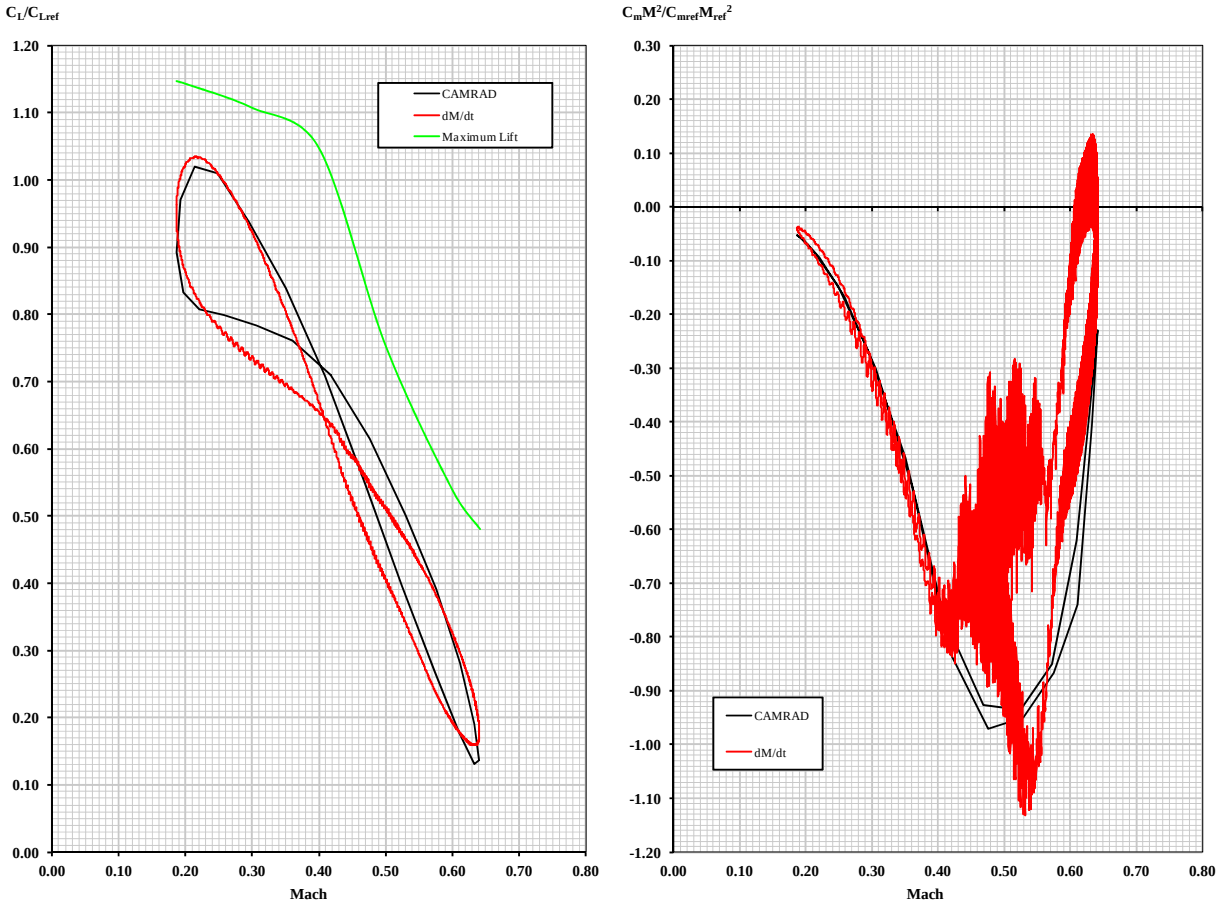

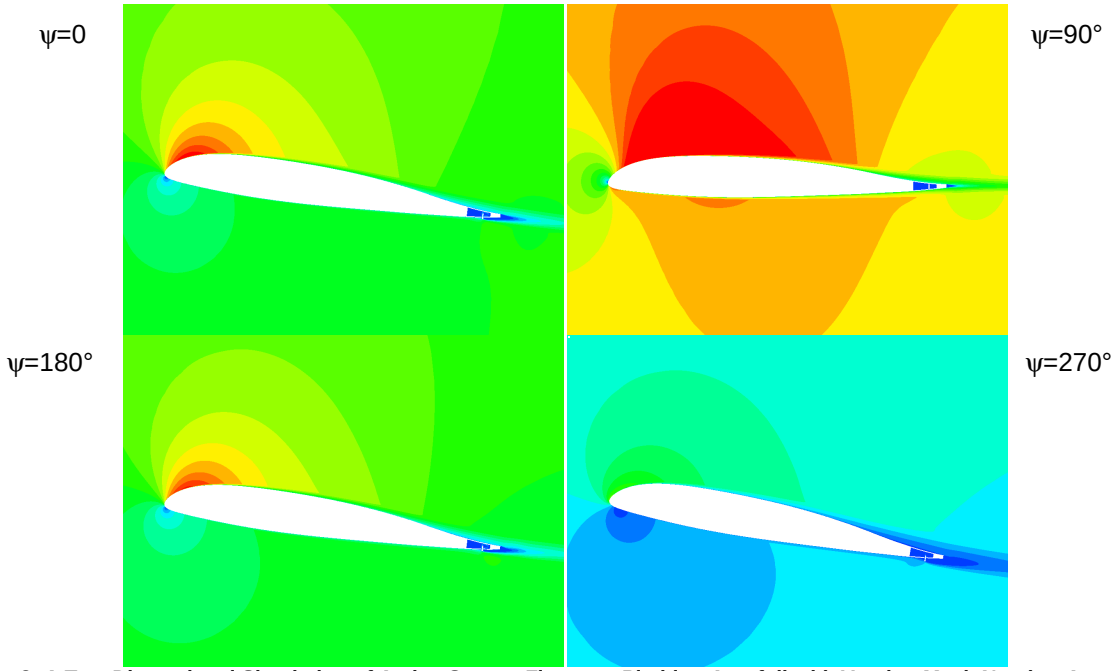

Figure 8: A Two Dimensional Simulation of Active Gurney Flap on a Pitching Aerofoil with Varying Mach Number Around the Azimuth Compared with CAMRAD Simulations at the Same Conditions, and Mach Number Contours around the Azimuth.

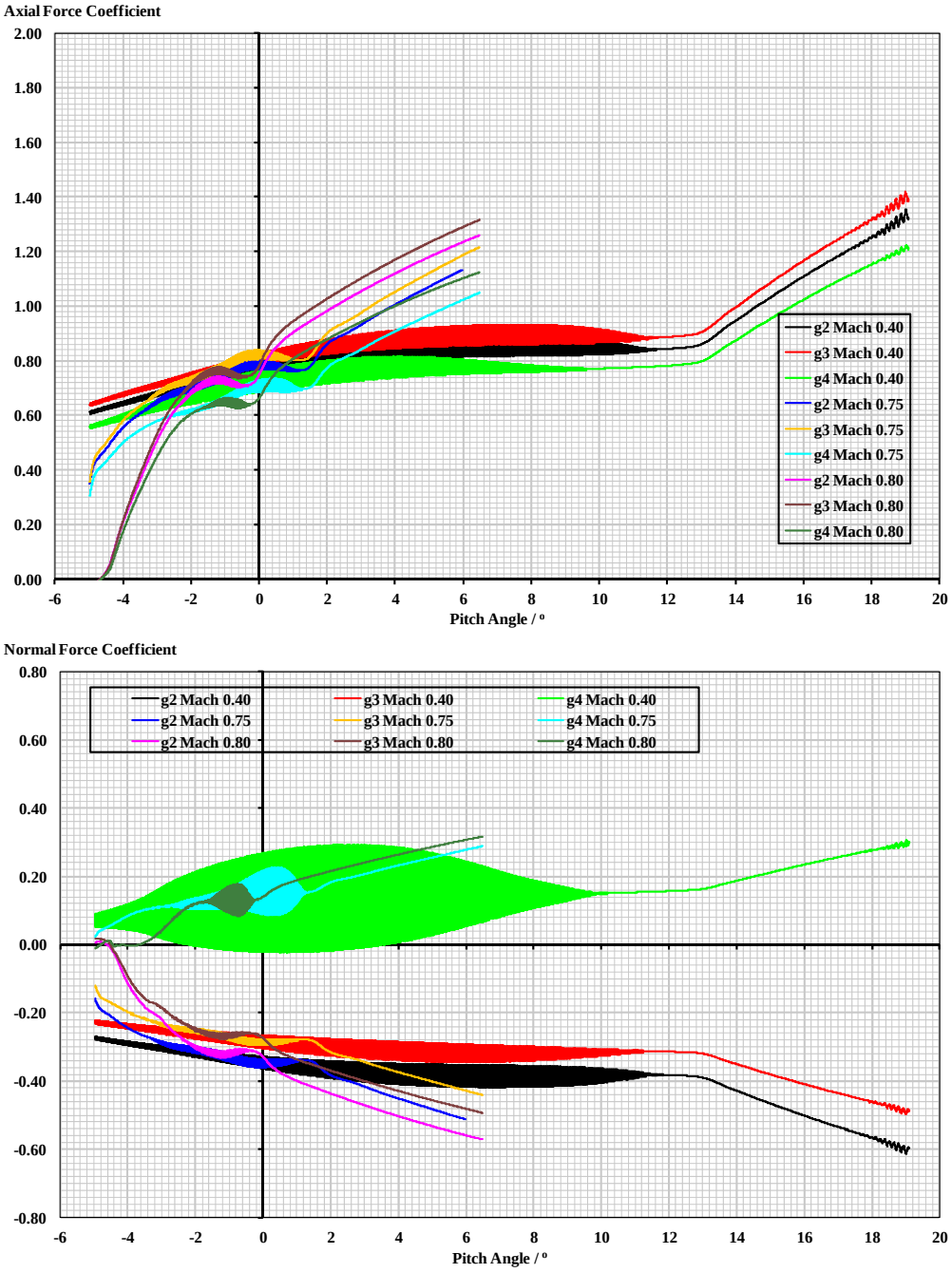

Figure 9: Axial and Normal Load Coefficients on 1% Deployed Gurney Flap, for Three Different Configurations of Internal Geometry and Gaps, based on Freestream Conditions and Gurney Height for the Axial Load and Gurney Thickness for the Normal Load.